Dual-cavity Fiber Fabry-Perot Interferometer Coated with SnO_2 for Relative Humidity and Temperature Sensing

Carmen E. Domínguez-Flores, Osvaldo Rodríguez-Quiroz, David Monzón-Hernández *Member, IEEE*, Joaquín Ascorbe, Jesús M. Corres *Member, IEEE*, and Francisco J. Arregui *Member, IEEE*

***Abstract*—An optical fiber tip interferometer for the measurement of relative humidity (RH) and temperature is proposed. The optical fiber structure used, a dual-cavity optical fiber Fabry-Perot interferometer (DFFPI), is simply-to-fabricate, compact, and robust. The reflectance (R_{DFFPI}) of the interferometer is sensitive to the refractive index (RI) and temperature of the external medium. Consequently, when the cross-section of the fiber tip was coated with a SnO_2 thin film, whose RI changes according to the humidity of the surrounding ambient, the measurement of the RH was possible. An increment of the RH produced a decrement of RI of the SnO_2 thin film, then the reflectance of the fiber tip end-face diminished, and this produced a decrement of the visibility of the interference fringes. The analysis of the R_{DFFPI} was carried out in the Fourier domain, using a novel processing method it was possible to establish that the amplitude of two peaks of Fourier spectrum changed at a ratio of 39.49×10^{-3} $\%RH^{-1}$ in the range of 40 to 90 RH%. On the other hand, the temperature of the humidity chamber was monitored, from 25 to 60 °C at a fixed RH%, by analyzing the phase shift of the interference pattern produced by the changes in the optical path length of the cavities. The good sensitivity, stability, reproducibility, and compactness of the fiber tip RH sensor make this proposal very appealing in a wide range of applications.**

***Index Terms*— Dual sensor, Fabry-Perot interferometer, Fourier Transform, Relative humidity, temperature**

I. Introduction

RELATIVE humidity is defined as a percentage ratio of the current absolute humidity to its maximum value under the same temperature conditions [1]. The accurate measurement of RH is crucial for the precise control of different processes in several strategic fields such as health [2], food processing [3], agriculture [4], or electronic manufacturing [5]. Nowadays, the electronic versions of the RH sensor are commonly used in industry due to its availability and low-cost. However, the response of this kind of sensors is significantly disturbed by the high level of electromagnetic noise present in most industrial environments, affecting the performance and durability of the sensors. Besides, the size of most of the electronic sensors, ranging from few to tens of millimeters, could limit their use. Some of these drawbacks are difficult to overcome and have opened the door to other technologies such as optical sensors. Among them those based on optical fiber technology have demonstrated a good capacity in dealing with these limitations. Other advantages of the fiber-optic sensors over their electronic counterparts are the high sensitivity, lightness, capability for multiplexing and remote sensing [6]. Furthermore, they are biocompatible, allowing them to be used in bio-medical sensing applications within the human body. In recent years, an important number of optical fiber sensors to measure RH have been proposed, in reflection and transmission configurations, based on the optical absorbance, fluorescence, or evanescent field interaction using long-period gratings [7], fiber Bragg gratings [8], hetero-core fiber structures for multimode interference [9], core-exposed fiber [10], lossy mode resonances [11], fiber Mach-Zehnder interferometers [12], [13] and fiber Fabry-Perot interferometers (FFPI) [14]-[24]. Special attention has been paid to FFPI-based RH sensors since they are simple to fabricate, highly stables, and ultra-compact. An important number of high-performance RH sensors based on single and dual fiber Fabry-Perot interferometers (FFPI and DFFPI) has been proposed using single-mode [15], [16], microstructure [17], photonic crystal [18], four-holes suspended-core [19], or multimode [20] fibers. In these approaches fibers have been coated with RH-sensitive materials such as polymethyl methacrylate (PMMA) [15], polyvinyl alcohol (PVA) [18], optical adhesives [16], [19], [21], Nafion [20], and thin films of SnO_2 [17], [24], Al_2O_3 [22], or $TiO_2/SiO_2/TiO_2$ [23]. Some of these schemes were also capable to sense temperature simultaneously [17–19], however, both parameters were monitored by tracking the phase shift of the interference pattern. The analysis of the changes in the reflectance of the FFPI, due to changes in the RH of the surrounding environment, has been traditionally carried out in

This work was supported by the Consejo Nacional de Ciencia y Tecnología (CONACyT) from Mexico under the CIENCIA BÁSICA under Project 257046 and Project LN-293442, and the Spanish Agencia Estatal de Investigación (AEI) and Fondo Europeo de Desarrollo Regional (FEDER) (TEC2016-79367-C2-2-R). The work of C. E. Domínguez-Flores and O. Rodríguez-Quiroz were supported by CONACyT for Ph.D. scholarship. *(Corresponding author: David Monzón-Hernández.)*

C. E. Domínguez-Flores, O. Rodríguez-Quiroz, and D. Monzón-Hernández are with the Centro de Investigaciones en Óptica A. C., León 37150, Mexico (e-mail: carmendmz@cio.mx; osvaldorq@cio.mx; dmonzon@cio.mx).

J. Ascorbe is with Nadetech Innovations S.L, Polígono Arbide, Calle V Nave 4, 31110 Noáin (Navarra) Spain (e-mail: joaquin.ascorbe@unavarra.es).

J. M. Corres and F. J. Arregui are with Department of Electrical, Electronic and Communication Engineering, Public University of Navarra and Institute of Smart Cities, Public University of Navarra, 31006 Pamplona, Spain (e-mail: jmcorres@unavarra.es; parregui@unavarra.es).

wavelength domain, tracking the displacement of the peaks or valleys [13,14,17,22–25]. Unfortunately, wavelength tracking is complicated to use in the case of the DFFPI, or in general in devices where two or more interference spectra are superposed on an optical spectrum. For this kind of devices, the analysis of the spectrum in the Fourier domain have been resulted the best option [16].

In this work, we proposed and demonstrated an optical fiber sensor for the monitoring of RH using a DFFPI coated with SnO_2. The structure of the sensor head, a micrometric section of capillary fiber (CF) inserted between a lead-in single-mode fiber (SMF) and a micrometric piece of SMF, is straightforward and easy-to-fabricate. The cross-section of the SMF tip end-face was coated with SnO_2 thin film by sputtering. When fiber sensors were exposed to different RH conditions, the SnO_2 thin film suffered a change in its refractive index that modulated the intensity of the light reflected. Consequently, the reflectance (R_{DFFPI}) of the SnO_2-coated DFFPI, a wavelength modulated spectrum, exhibited a change in the interference fringe visibility. These changes are difficult to follow in the optical domain, therefore, each spectrum was transformed to Fourier domain. The typical spectrum of the DFFPI exhibited a series of peaks corresponding to the optical path lengths of each cavity. It was possible to establish a one-to-one relationship between the RH and the amplitude of two of the peaks. On the other hand, the temperature was monitored by analyzing the phase of the spectrum at a fixed value of the optical path length (OPL). This point sensor showed good sensibility and repeatability to RH and temperature, in the measurement range of 40 to 90% and 25 to 60 °C, respectively.

II. Fabrication and Characterization of the DFFPI

To fabricate the DFFPI a semi-automatic, portable and reconfigurable mechatronic platform was designed and constructed [26], this stage allowed to cleave optical fiber with micrometric precision. The fabrication process of the DFFPI is depicted in Fig. 1. Firstly, SMF (9/125) and CF (62/125) were spliced using a S123C (Furukawa Electric Co.) fusion splicer (Fig. 1(a)). Then, the ends of the fiber structure were fixed to a pair of PC controlled translation stages (MTS25-Z8, THORLABS), previously aligned and separated 40 cm approximately. The SMF and CF splice was set to coincide with the blade of the fiber cleaver (FC-6, Sumimoto Electric), placed between the translation stages. A digital camera, attached to a commercial 40X stereo microscope objective (Edmund Optics), was used to monitor the fiber position respect to the cleaver blade, used as a reference position. Fiber splice was displaced a distance L_1 and CF was cleaved (Fig. 1(b)). The first cavity was formed when a SMF was spliced to the CF as is illustrated in Fig. 1(c). The second cavity was formed when SMF was cleaved following the same aligning and cleaving process described previously. The final structure of the DFFPI, SMF-CF-SMF, is shown in Fig. 1(d).

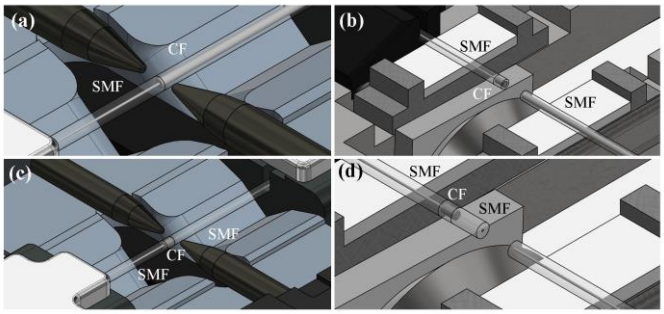

Fig. 1. Illustration of the DFFPI fabrication.

The intensity of the light reflected by the DFFPI (I_r) is described by Eq. 1, where it is possible to distinguish three interference terms. The three beams involved were generated by the interfaces SMF-CF, CF-SMF and SMF-external medium whose reflectivity are R_0, R_1, and R_2, respectively [27].

$$I_r = \left[R_0 + 2A(1-R_0)\sqrt{R_0R_1}\cos(2kL_1n_0+\pi) + 2A^2(1-R_0)^2(1-R_1)\sqrt{R_1R_2}\cos(2kL_1n_1+\pi) + 2A(1-R_0)(1-R_1)\sqrt{R_0R_2}\cos(2k(L_1n_0+L_2n_1)+\pi) + A^2(1-R_0)^2(1-R_1)^2R_2 + A^2(1-R_0)^2R_1\right]I_0 \quad (1)$$

I_0 is the intensity of light delivered by the lead-in SMF, n_0, L_1, and n_1, L_2 are the refractive index and length of the first (CF) and second (SMF) cavity, respectively. $A = (1-\alpha)$ represents the transmission loss coefficient. The wavenumber is represented by k, and the reflectivity of the first and second surface is calculated using $R_{0,1} = ([n_1 - n_0]/[n_1 + n_0])^2$. It is evident that I_r depends on the RI of the external medium (n_{ext}) since $R_2 = ([n_1 - n_{ext}]/[n_1 + n_{ext}])^2$ [27,28].

The characterization of the DFFPIs was made using a light source (Agilent 83437A) centered at 1550 nm, an Optical Spectrum Analyzer (OSA) HP86142A and an optical fiber circulator. The fiber tip was immersed in different Cargille oils with a calibrated RI. The experimental reflectance R_{DFFPI}, defined as $\frac{I_r}{I_0}$, obtained with one of the devices fabricated, $L_1 = 57.40\ \mu m$ and $L_2 = 261.32\ \mu m$, is shown in Fig. 2(a). It is evident that the fringe contrast of the modulation decreased when n_{ext} increases within the range $1 < n_{ext} \leq n_1$. When fiber tip facet was in contact with a Cargille oil with a RI higher than n_1, the contrast of the interference pattern increases. The amplitude of the peaks of the Fourier Transform (FT), calculated using the signal processing algorithm described in reference [29], is shown in Fig. 2(b). The maximum amplitude of the first, second and third peak, around the OPL value of 57, 261 and 318 μm, are referred as P_1, P_2 and P_3, respectively. It is important to notice that peaks of the Fourier spectra are not overlapped, this facilitate the individual analysis of the changes in the position and the amplitude of each peak due to external perturbations. The position of the peaks is directly related to the length of the interferometer cavities. The length of the first cavity was decided to be larger than 50 μm to ensure that position of the first peak was far from the *y*-axis in Fourier spectrum. In order to avoid the overlapping of first and second peaks the length of the second cavity should be at least two times larger than that of the first cavity [30]. The calibration

curve shown in Fig. 2 (c) was constructed by calculating the ration $R_{Amplitude} = \frac{P_3}{P_1{}^{air}}$, $P_1{}^{air}$ is the maximum of peak 1 amplitude when DFFPI was surrounded by air. The ambiguous behavior of the curve, i.e. two different values of n_{ext} produce the same $R_{Amplitude}$ value, is the main drawback of the Fresnel reflection-based fiber interferometers.

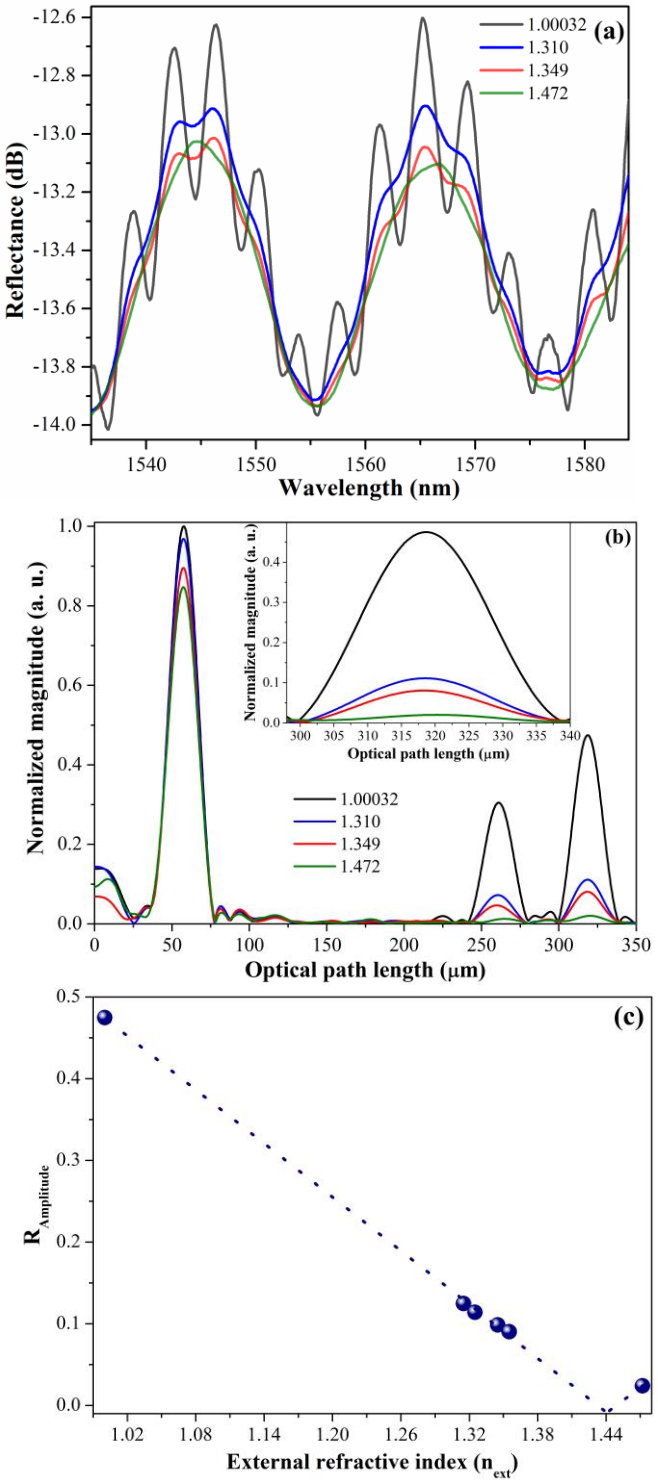

Fig. 2. Experimental spectra of the R_{DFFPI} in (a) the optical and (b) Fourier domain obtained for four different Cargille oils. (c) Characterization curve of the DFFPI, representing the evolution of the $R_{Amplitude}$ respect to changes of n_{ext}.

III. SENSING PRINCIPLE OF THE DFFPI COATED WITH A HUMIDITY-SENSITIVE LAYER

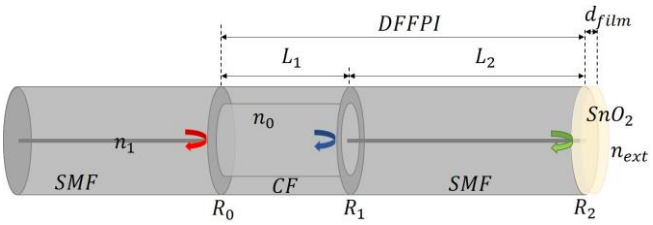

Fig. 3. Representation of a DFFPI with a thin film of SnO_2 deposited over the fiber tip end-face.

It has been demonstrated that R_{DFFPI} is dependent on the reflectance of the end-face of the fiber tip interferometer, which can be modified by changing the RI of the fiber tip surrounding media [27-29]. This property was exploited to demonstrate DFFPI-based humidity sensors, by simply covering the fiber tip end-face with a material whose RI is dependent on the RH of the surrounding environment. Among the number of humidity-sensitive materials used so far [15-23], tin oxide possesses unique optical properties, such as high optical transparency in a wide spectral band [31]. Furthermore, at low concentrations this material exhibits an excellent chemical stability and low toxicity [2]. However, the most important feature for sensing applications is the capacity to vary its optical properties under the presence of some gases [32–34] or changes in humidity conditions [11,16,35,36]. The humidity sensitivity of SnO_2 is related to the presence of oxygen species on the surface, produced by the physisorption and capillary condensation of water molecules on the surface of the material when RH increases [37], [38].

The schematic representation of the DFFPI coated with SnO_2 thin film proposed for RH sensing is showed in Fig 3. The I_r of the DFFPI coated with SnO_2 is described by the equation (1) but the reflectance of the last surface is described by [39]:

$$R_2 = \left| \frac{r_{12} + r_{23} \cdot e^{-i \cdot k_{film}}}{1 + r_{12} r_{23} \cdot e^{-i \cdot k_{film}}} \right|^2 \quad (2)$$

with

$$r_{12} = \frac{n_1 - n_{film}}{n_1 + n_{film}}; \; r_{23} = \frac{n_{film} - n_{ext}}{n_{film} + n_{ext}}; \; k_{film} = \frac{4\pi \cdot n_{film} \cdot d_{film}}{\lambda} \quad (3)$$

Where n_{film} and d_{film} are the refractive index and thickness of the SnO_2 film. It can be observed that the reflected intensity is dependent on the thickness and RI of the thin film and the RI of the external medium. Since the RI of SnO_2 is modified by humidity conditions it is feasible to monitor the humidity changes by measuring the reflected intensity of the DFFPI. In order to corroborate this hypothesis a series of experiments with DFFPI coated with tin oxide thin film were carried out. Firstly, a DFFPI, with cavity lengths of $L_1 = 57.40\,\mu m$ and $L_2 = 261.32\,\mu m$, was introduced in the vacuum chamber of the sputtering machine (Pulsed DC-Sputtering System Nadetech Inc.) and coated with tin oxide. SnO_2 with a purity of 99.99% was purchased from ZhongNuo Advanced Material Technology Co. The sputtering process was done at 9x10-

^{3} mbar and 90 mA for 20 seconds. In order to monitor the evolution of the reflectance of the DFFPI during the sputtering process, the device was spliced to the second port of an optical fiber circulator, the first and third ports were used to connect the light source and the OSA, respectively.

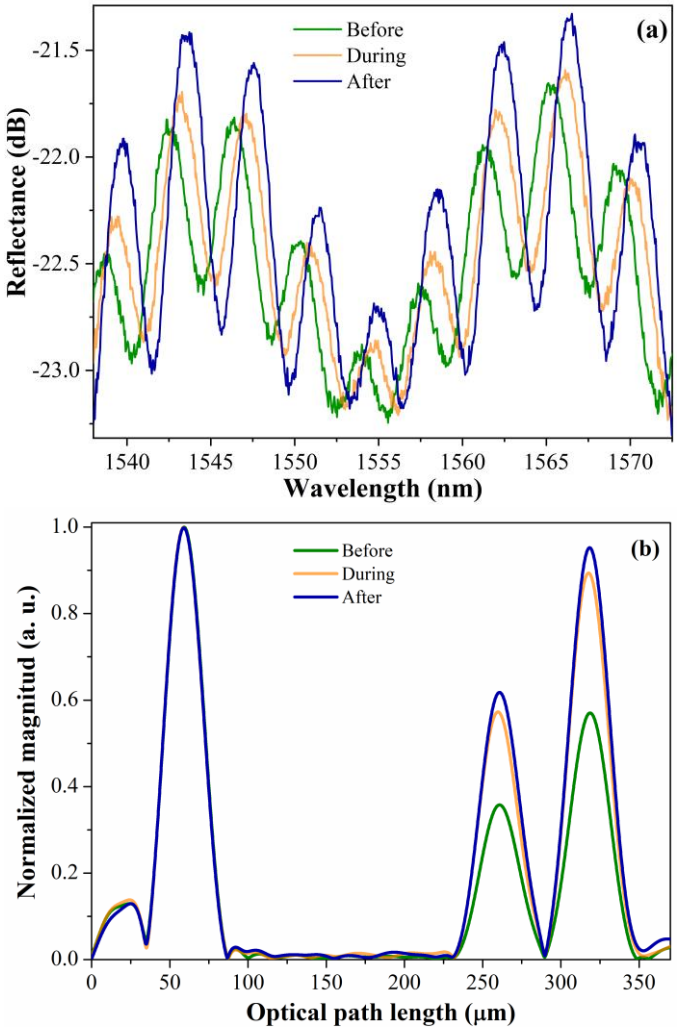

Fig. 4. (a) Experimental spectra of the DFFPI reflectance during the SnO_2 deposition. (b) The Fourier spectra of the experimental signal.

The spectra of the reflectance, shown in Fig. 4(a), were recorded before (green graph), during (orange graph) and after (blue graph) the sputtering process. The final interference pattern exhibited a red shift and a notorious increment on the fringe visibility. Those spectra were transformed to Fourier domain and are shown in Fig. 4(b). A considerable increment in the amplitude of the last two peaks, before and after the coating process, is observed. This is due to the increment of reflectivity (R_2 in Fig. 3) of the fiber tip facet due to the deposition of the SnO_2 thin film.

In the theoretical model of the SnO_2-coated DFFPI, described by Eqs. (1)-(3), the reflectance of the last surface (R_2) depends on the refractive index of external medium, among other parameters. After the coating process, the device was immersed in different Cargille oils with refraction indexes between 1.296 and 1.482, at room temperature, in order to demonstrate that R_2 can be modulated by external medium. The reflectance in the Fourier domain when DFFPI is presented in Fig. 5(a). The augment of the external medium refractive index produced a gradual decrement of the amplitude of peaks 2 and 3. According to Eq. (3) the diminution of R_2, that produced the decrement of peaks 2 and 3, will continue while $n_{ext} \leq n_{film}$. The calibration curve showed in Fig. 5(b) was obtained by calculating $R_{Amplitude}$, where it is possible to observe a noticeable increment in the original RI measurement range of the DFFPI from [1, 1.447] to [1, 1.482], but the theoretical limit is even larger [1, n_{SnO_2}] since according to Ref. [40] n_{SnO_2} =1.85.

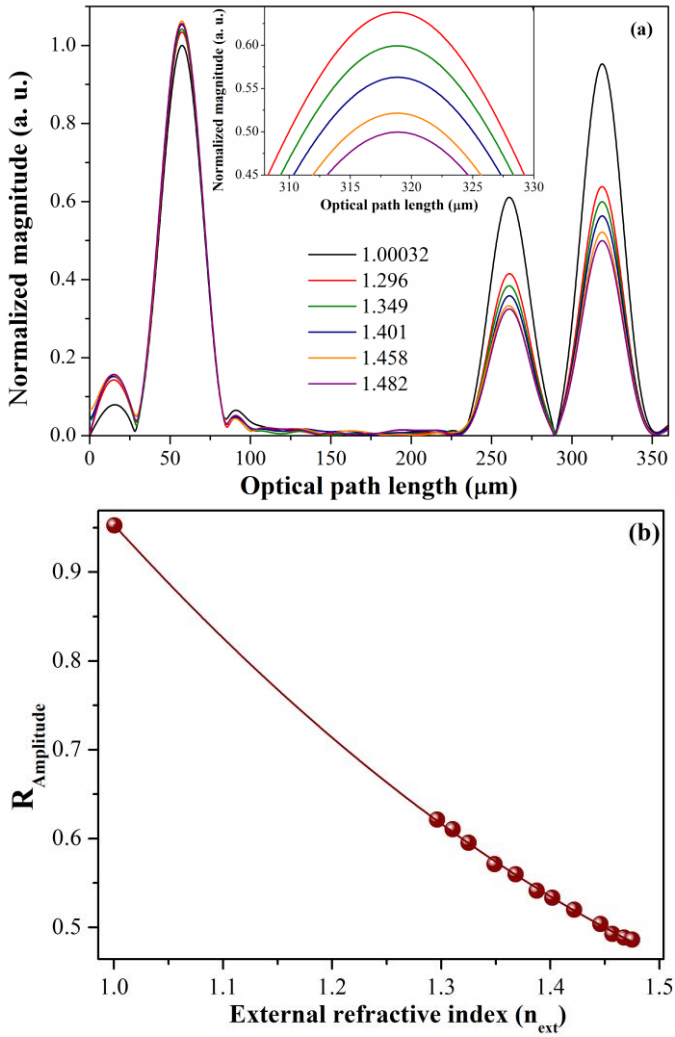

Fig. 5. (a) Fourier transform of the reflected spectra obtained when DFFPI coated with SnO_2 was immersed in oils with different RI. (b) Refractometric curve response of the device.

IV. Experimental Results and Discussion

The experimental setup used to test the response of the DFFPIs coated with SnO_2 to RH changes is shown in Fig. 6, each fiber tip was introduced in a climatic chamber (Angelantoni Industries ACS CH 250) and then connected to a 3-port optical fiber circulator.

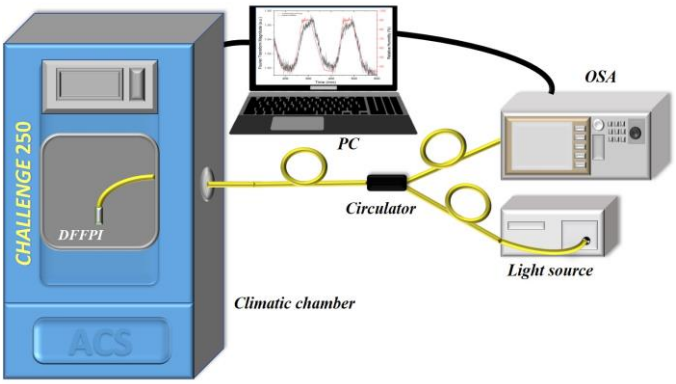

Fig. 6. Experimental setup for relative humidity measurements.

The length of the first and the second cavity of the first (DFFPI-1) and second (DFFPI-2) device were $L_1 = 57.40\ \mu m$, $L_2 = 261.32\ \mu m$ and $L_1 = 65.14\ \mu m$, $L_2 = 240.23\ \mu m$ respectively. The sputtering process of the DFFPI-1 lasted 20 seconds while for the DFFPI-2 was 30 seconds. Based on the analysis of the time-deposition and the thickness-size made on Ref. [13] where the same technique, material and sputtering machine were used. We estimated that the thickness of the SnO_2 film deposited over the DFFPI-1 and -2 was 28 and 43 nm, respectively. Since the sputtering parameters and the position of the fiber tip inside the chamber were exactly the same for both samples, the thickness of the SnO_2 thin film of the DFFPI-2 was thicker. The DFFPIs coated with SnO_2 were exposed to different humidity conditions at a fixed temperature for 1000 minutes. During the test, the optical reflectance of the devices was recorded every 20 seconds. Each spectrum of the reflectance was transformed into a Fourier domain and $R_{Amplitude}$ was calculated. Since the $R_{Amplitude}$ was inversely proportional to the RH, the inverse of the $R_{Amplitude}$ was used to represents the devices response to different humidity conditions. Several cycles from 40 to 90 RH% were applied to the devices in the climatic chamber while the temperature was kept constant to 25 °C. One of these cycles is shown in the black graph of the inset of Fig. 7(a) and 7(b), for DFFPI-1 and DFFPI-2, respectively. The responses of the DFFPIs (red graph) are compared with the climatic chamber sensor (an electronic sensor). The response of both devices is different, the response of the DFFPI-2 (Fig. 7(b)) is one order of magnitude larger than that observed with the DFFPI-1, the device with thinner film. It can be said that sensor sensitivity is directly dependent on the thin film thickness. The sensor response for the increments (blue points) and decrements (green points) of the RH are shown in Fig. 7(a) and 7(b). It can be clearly seen that the dispersion of the experimental points, that represent the signal delivered by the sensors at a particular RH, is larger in the case of the DFFPI-1 (Fig. 7(a)). This means that the uncertainty to determine the RH of the medium is larger in the device with the thinner SnO_2 film. The temperature response of the DFFPI-1 was measured in the range between 25 and 60 °C while the RH was kept constant to 38%. Temperature changes affect the dimensions of the cavity length of the fiber interferometer; the increment or decrement produces a slight shift in the optical spectrum that can be measured by analyzing the changes of the FT phase. Such changes can be seen in Fig. 7(d), obtained with the first device. Another important advantage of the sensors proposed here is that RH and temperature are measured by using two independent parameters of the sensor signal.

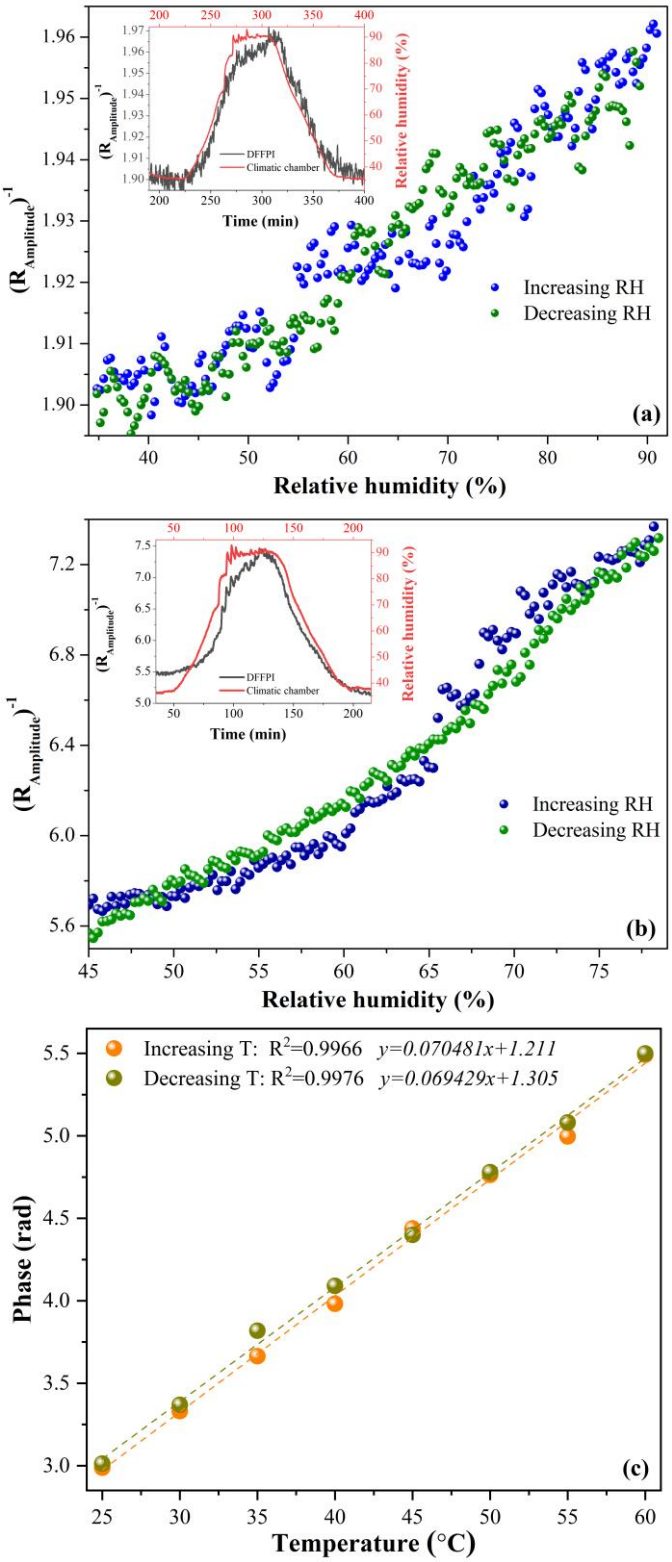

Fig. 7. Relative humidity response of (a) DFFPI-1 with thinner and (b) DFFPI-2 with thicker SnO_2 thin film. The temporal response of the DFFPIs, compared with the response an electronic sensor, are shown in the insets of (a) and (b). (c) Temperature monitoring of the DFFPI-1while the RH was fixed.

V. Conclusions

A simple-to-fabricate, robust, and compact optical fiber for the measurement of RH was proposed and demonstrated. The sensor head consisted of a DFFPI coated with SnO_2 thin film, deposited over the fiber tip by sputtering. The operation principle of the RH sensor is based on the changes of reflectance of a SnO_2 thin film deposited over the fiber tip enface. Such changes produced an alteration of the visibility of the interference pattern that was monitored through the amplitude of the peaks of the Fourier spectra. On the other hand, it was observed that temperature changes produced a displacement of the interference pattern monitored as the variations in the phase of the Fourier spectra. The dynamic range for RH and temperature of the sensors was 40 to 90 RH % and 25 to 60°C, respectively. All these features make this proposal very attractive for real-world applications.

Acknowledgments

The authors are grateful to the Consejo Nacional de Ciencia y Tecnología (Mexico) for financial support through the projects CB 257046 and LN 293442. This work was also supported by the Spanish Agencia Estatal de Investigación (AEI) and Fondo Europeo de Desarrollo Regional (FEDER) (TEC2016-79367-C2-2-R). C. E. Domínguez-Flores and O. Rodríguez-Quiroz want to thank CONACyT for their support through a Ph.D. scholarship.

References

[1] W. Xu, W. Bin Huang, X. G. Huang, and C. Y. Yu, "A simple fiber-optic humidity sensor based on extrinsic Fabry-Perot cavity constructed by cellulose acetate butyrate film," *Opt. Fiber Technol.*, vol. 19, no. 6 PART A, pp. 583–586, 2013.

[2] J. Hromadka et al., "Simultaneous in situ temperature and relative humidity monitoring in mechanical ventilators using an array of functionalized optical fibre long period grating sensors," *Sensors Actuators B. Chem.*, vol. 286, no. June 2018, pp. 306–314, 2019.

[3] A. C. L. Wong, "Biofilms in Food Processing Environments," *J. Dairy Sci.*, vol. 81, no. 10, pp. 2765–2770, 1998.

[4] S. Y. Park, S.-Y. Choi, and S.-D. Ha, "Predictive Modeling for the Growth of Aeromonas hydrophila on Lettuce as a Function of Combined Storage Temperature and Relative Humidity," *Foodborne Pathog. Dis.*, vol. 16, no. 6, pp. 376–383, 2019.

[5] R. Ciprian and B. Lehman, "Modeling effects of relative humidity, moisture, and extreme environmental conditions on power electronic performance," *2009 IEEE Energy Convers. Congr. Expo. ECCE 2009*, pp. 1052–1059, 2009.

[6] M. Yin, B. Gu, Q. An, C. Yang, Y. Liang, and K. Yong, "Recent development of fiber-optic chemical sensors and biosensors: Mechanisms, materials, micro/nano-fabrications and applications," *Coord. Chem. Rev.*, vol. 376, pp. 348–392, 2018.

[7] A. Urrutia, J. Goicoechea, A. L. Ricchiuti, D. Barrera, S. Sales, and F. J. Arregui, "Simultaneous measurement of humidity and temperature based on a partially coated optical fiber long period grating," *Sensors Actuators B Chem.*, vol. 227, pp. 135–141, 2016.

[8] P. Kronenberg, P. K. Rastogi, P. Giaccari, and H. G. Limberger, "Relative humidity sensor with optical fiber Bragg gratings," *Opt. Lett.*, vol. 27, no. 16, pp. 1385–1387, 2002.

[9] W. Xu and J. Shi, "Relative Humidity Sensor Based on No-Core Fiber Coated by Agarose-Gel Film," *Sensors*, vol. 17(10), pp. 1–9, 2017.

[10] D. Gomez, S. P. Morgan, B. R. Hayes-gill, R. G. Correia, and S. Korposh, "Chemical Polymeric optical fibre sensor coated by SiO_2 nanoparticles for humidity sensing in the skin microenvironment," *Sensors Actuators B. Chem.*, vol. 254, pp. 887–895, 2018.

[11] J. Ascorbe, J. M. Corres, I. R. Matias, and F. J. Arregui, "High sensitivity humidity sensor based on cladding-etched optical fiber and lossy mode resonances," *Sensors Actuators B Chem.*, vol. 233, pp. 7–16, 2016.

[12] Y. Zhong, Z. Tong, W., Juan Qin and W. Gao, "Humidity and temperature sensor based on a Mach – Zehnder interferometer with a pokal taper and peanut taper," *Appl. Opt.*, vol. 58, no. 29, pp. 7981–7986, 2019.

[13] D. Lopez-Torres, C. Elosua, J. Villatoro, J. Zubia, M. Rothhardt, K. Schuster, F.J. Arregui, "Enhancing sensitivity of photonic crystal fiber interferometric humidity sensor by the thickness of SnO_2 thin films," *Sensors Actuators B Chem.*, vol. 251, pp. 1059–1067, 2017.

[14] C. Lang, Yi Liu, K. Cao, Yan Li and S. Qu, "Ultra-compact, fast-responsive and highly-sensitive humidity sensor based on a polymer micro-rod on the end-face of fiber core," *Sensors Actuators B Chem.*, vol. 290, pp. 23-27, 2019.

[15] O. Arrizabalaga, J. Velasco, J. Zubia, I. Sáez, D. Ocáriz, and J. Villatoro, "Miniature interferometric humidity sensor based on an off-center polymer cap onto optical fiber facet," *Sensors Actuators B Chem.*, vol. 297, p. 126700, 2019.

[16] A. Lopez Aldaba et al., "SnO_2-MOF-Fabry-Perot optical sensor for relative humidity measurements," *Sensors Actuators B Chem.*, vol. 257, pp. 189–199, 2018.

[17] H. Sun, X. Zhang, L. Yuan, L. Zhou, X. Qiao, M. Hu, "An Optical Fiber Fabry–Perot Interferometer Sensor for Simultaneous Measurement of Relative Humidity and Temperature," *IEEE Sensors Journal*, vol. 15, pp. 2891-2897, 2014.

[18] C. Wang, G. Yan, Z. Lian, X. Chen, S. Wu, and S. He, "Hybrid-cavity fabry-perot interferometer for multi-point relative humidity and temperature sensing," *Sensors Actuators B Chem.*, vol. 255, pp. 1937–1944, 2018.

[19] E. Maciak, "Low-Coherence Interferometric Fiber Optic Sensor for Humidity Monitoring Based on Nafion ® Thin Film ," *Sensors*, vol. 19(3), pp. 629, 2019.

[20] R. Oliveira, L. Bilro, T. H. R. Marques, and C. M. B. Cordeiro, "Simultaneous detection of humidity and temperature through an adhesive based Fabry – Pérot cavity combined with polymer fiber Bragg grating," *Opt. Lasers Eng.*, vol. 114, pp. 37–43, 2019.

[21] S. Liu, Y. Ji, J. Yang, W. Sun, H. Li, "Nafion film temperature/humidity sensing based on optical fiber Fabry-Perot interference," *Sensors Actuators A: Phys.*, vol. 269, pp. 313–321, 2018.

[22] C. Huang, W. Xie, M. Yang, J. Dai, B. Zhang, and S. Member, "Optical Fiber Fabry – Perot Humidity Sensor Based on Porous Al_2O_3 Film," *IEEE Photonics Technology Letters*, vol. 27, no. 20, pp. 2127–2130, 2015.

[23] C. Huang, W. Xie, D. Lee, C. Qi, M. Yang, M. Wang, J. Tang, "Optical fiber humidity sensor with porous $TiO_2/SiO_2/TiO_2$ coatings on fiber tip," *IEEE Photon.Technol.Lett.*, vol. 27(14), pp. 1495-1498, 2015.

[24] J. Ascorbe, C. Sanz, J. M. Corres, F. J. Arregui, and R. Matías, "High sensitivity extrinsic Fabry-Pèrot interferometer for humidity sensing," *9th International Conference on Sensing Technology (ICST)*, no. 1, pp. 143–146, 2015.

[25] C. Bian, M. Hu, R. Wang, T. Gang, R. Tong, L. Zhang, T. Guo, X. Liu, X. Qiao, "Optical fiber humidity sensor based on the direct response of the polyimide film," *Appl. Opt.*, vol. 57, no. 2, p. 356, 2018.

[26] C.E. Dominguez-Flores, J. Basulto, D. López-Cortés, and D. Monzón-Hernández, "Semi-automatic Platform for Fabry-Perot Microcavities Construction," *Progress in Optomechatronic Technologies*, pp. 135–140, 2019.

[27] Z. L. Ran, Y. J. Rao, W. J. Liu, X. Liao , and K. S. Chiang, "Laser-micromachined Fabry-Perot optical fiber tip sensor for high-resolution temperature-independent measurement of refractive index," *Opt. Express*, vol. 16, no.3, pp. 2252-2263, 2008.

[28] B. Xu, Y. Yang, Z. Jia, and D. N. Wang, "Hybrid Fabry-Perot interferometer for simultaneous liquid refractive index and temperature measurement," *O-pt. Express*, vol. 25, no. 13, pp. 14483–14493, 2017.

[29] O. Rodriguez-Quiroz, C. E. Dominguez-Flores, D. Monzón-Hernandez, and C. Moreno-Hernandez, "Hybrid Fiber Fabry–Perot Interferometer With Improved Refractometric Response," *J. Light. Technol.*, vol. 37, no. 17, pp. 4268–4274, 2019.

[30] O. Rodriguez-Quiroz, C. E. Dominguez-Flores, D. Monzon-Hernandez, E. Morales-Narvaez, V. P. Minkovich, D. Lopez-Cortes, "Unambiguous refractive-index measurement in a wide dynamic-range using a hybrid fiber Fabry-Perot interferometer assisted by a fiber Bragg grating,", Opt. Laser Technol., vol. 128, 106236 1-8, 2020.

[31] J. Koshy et al., "Optical properties of SnO_2 nanoparticles Optical Properties of SnO_2 Nanoparticles," *AIP Conference Proceedings 1620*, vol. 192, no. 2014, pp. 2–7, 2015.

[32] T. Seiyama, A. Kato, K. Fujiishi, and M. Nagatani, "A New Detector for Gaseous Components Using Semiconductive Thin Films.," *Anal. Chem.*, vol. 34, no. 11, pp. 1502–1503, 1962.
[33] N. Ma, K. Suematsu, M. Yuasa, T. Kida, and K. Shimanoe, "Effect of Water Vapor on Pd-Loaded SnO_2 Nanoparticles Gas Sensor," *ACS Applied Materials \& Interfaces*, vol. 7, pp. 5863-5869, 2015.
[34] N. Bârsan and U. Weimar, "Understanding the fundamental principles of metal oxide-based gas sensors; the example of CO sensing with SnO_2 sensors in the presence of humidity," *Journal of Physics: Condensed Matter*, vol. 813, 2003.
[35] Q. Kuang, C. Lao, Z. L. Wang, Z. Xie, and L. Zheng, "High-Sensitivity Humidity Sensor Based on a Single SnO_2 Nanowire," *J. Am. Chem. Soc.*, pp. 6070–6071, 2007.
[36] H. Liu et al., "Relative Humidity Sensor Based on S-Taper Fiber Coated With SiO_2 Nanoparticles," *IEEE Sensors Journal*, vol. 15, no. 6, pp. 3424–3428, 2015.
[37] V. A. Gercher and D. F. Cox, "Water adsorption on stoichiometric and defective SnO_2(110) surfaces," *Surface Science*, vol. 322(1) pp. 177-184, 1995.
[38] P. M. Faia and C. S. Furtado, "Effect of composition on electrical response to humidity of TiO_2:ZnO sensors investigated by impedance spectroscopy," *Sensors Actuators B Chem.*, vol. 181, pp. 720–729, 2013.
[39] M. Consales, A. Buosciolo, A. Cutolo, G. Breglio, A. Irace, S. Buontempo, P. Petagna, M. Giordano, A. Cusano, "Fiber optic humidity sensors for high-energy physics applications at CERN," *Sensors Actuators B. Chem.*, vol. 159, no. 1, pp. 66–74, 2011.
[40] J. Ascorbe, J. M. Corres, I. del Villar and I. R. Matias, "Fabrication of long period gratings by periodically removing the coating of cladding-etched single mode optical fiber towards optical fiber sensor development," *Sensors*, vol. 18 pp. 1866, 2018.

Carmen E. Domínguez-Flores was born in Saltillo, Mexico, in 1992. She received the B.S. degree in physics engineering from Universidad Autónoma de Coahuila in 2016 and the M.Sc. degree from Centro de Investigaciones en Óptica (CIO) A., C. in 2018, where she is currently pursuing the Ph.D. degree in optical science. Her research interests include fiber optic sensors and fiber Fabry–Perot interferometers.

Osvaldo Rodríguez-Quiroz was born in Manuel Doblado, México. He received the B.Eng. degree in communications and electronics in 2001 and the M.Eng. degree in electrical engineering from the University of Guanajuato, Guanajuato, Mexico, in 2004. In 2016, he joined the Research Center in Optics (CIO), where he is currently working toward the Ph.D. degree working on the simultaneous measurement of the refractive index and temperature for the monitoring and analysis of fluids. His research interests include fiber-optic sensors and digital signal processing.

David Monzón-Hernández received the Ph.D. degree from the Universidad of Guanajuato, Mexico, in 1999. Since 2002, he has been a Research Fellow with the Centro de Investigaciones en Óptica (CIO) A. C. He is currently involved in the design and fabrication of optical fiber devices and sensors. His research interests include optofluidics, plasmonics, and biosensors.

Joaquín Ascorbe received the M.S. degree in electrical engineering and the Ph.D. degree from the Public University of Navarra (UPNA), Spain, in 2012 and 2018, respectively. Since then he has been involved in research projects related to optical fiber sensors and nanodeposition technologies. In 2014 he held the Fundación Fuentes Dutor research grant for the development of optical fiber sensors for the electrical power network. He is currently working in Nadetech Innovations and his main interest is related to the different coating techniques, especially those related to vacuum deposition.

Jesus M. Corres received the M.S. and Ph.D. degrees in electrical and electronic engineering from the Public University of Navarra, Pamplona, Spain, in 1996 and 2003 respectively. He is an Associate Professor with the Electrical and Electronic Engineering Department and vice-principal of the Industrial Engineering, Computing and Telecommunications School, Public University of Navarre and has been involved in different projects with industry including power systems design and motion control. He is Associate Editor of "IEEE Sensors Letters" and MDPI "Sensors". His main research interests include optical fiber sensors and nanostructured materials and he is co-founder of two technology companies.

Francisco J. Arregui is Vice-President of Research at the Public University of Navarra, Pamplona, Spain. He was part of the team that fabricated the first optical fiber sensor by means of the layer-by-layer nano-assembly method at Virginia Tech, Blacksburg, VA, USA, in 1998. He is the author of more than 180 scientific journal papers and 200 conference publications (cited more than 6500 times, h-index of 44, Scopus), most of them related to optical sensors based on nanostructured coatings. Prof. Arregui has been Founding Editor-in-Chief of "Journal of Sensors" as well as Associate Editor or Guest Editor of "Sensors", "IEEE Journal of Selected Topics in Quantum Electronics", "IEEE Sensors Journal", "Journal of Sensors" and "International Journal on Smart Sensing and Intelligent Systems". Dr. Arregui regularly cooperates as evaluator for Science Agencies of different countries as well as participates in the Technical Program Committee of sensor-related conferences (IEEE Sensors, Eurosensors, Transducers, CLEO Europe, ICST). He has been Opening Plenary Speaker of Eurosensors and is also editor of the books "Sensors based on nanostructured materials" and "Optochemical Nanosensors", co-inventor of 14 patents and co-founder of 5 technology-based companies, among them, Iden Biotechnology S.L.; EverSens S.L.; Pyroistech S.L and Nadetech Innovations S.L.